A Constitutive Model for the Simulation of Fabric-Reinforced Materials under Automotive Crash Conditions

Eduardo Martin-Santos[1,2], Alejandro Dominguez[1], Alfredo Alameda[1], Ángel Sillero[1], Tomohiko Max Miura[3]

[1]Applus IDIADA
[2]Civil and Environmental Engineering Department (DECA), ETSECCPB, Universidad Politècnica de Catalunya (UPC), Campus Nord, 08034 Barcelona, Spain
[3]TOYOTA GAZOO Racing Europe GmbH, Toyota Allee 7, 50858 Cologne, Germany

1 Introduction

Automotive regulations are continuously evolving, becoming increasingly stringent regarding environmental impact and safety requirements. This evolution compels manufacturers to explore innovative approaches for producing more efficient and safer vehicles. Within this context, lightweighting by Multi-Material philosophy has emerged as one of the most promising strategies: a systematic approach to reduce vehicle mass without compromising safety, comfort, or functionality. To maintain or enhance safety standards, lightweight structures necessitate higher performance specifications, driving the application of innovative materials with superior specific properties [1]. In safety-critical applications, where materials must perform effectively during impact events, Specific Energy Absorption (SEA) becomes a crucial parameter for material selection.

The substitution of conventional mild steel structural components with a combination of advanced materials has consequently gained significant importance for optimizing lightweighting. Composite materials offer the required weight reduction while maintaining or even enhancing energy absorption during crash events. Unlike traditional mild steels, where energy absorption occurs primarily through plastic deformation, composite materials dissipate energy through complex damage mechanisms, generating numerous fractures in both fibre and matrix due to the initiation and progression of simultaneous, interacting failure processes.

Composite materials demonstrate particularly significant potential in Electric Vehicles (EVs), where battery systems can constitute approximately 30% of the vehicle weight, necessitating structural mass reduction elsewhere. In these applications, composite materials additionally provide superior thermal insulation and electromagnetic shielding properties.

Despite these advantages, integrating composite materials into automotive engineering presents several challenges. Cost remains a significant barrier, particularly for mass-market vehicles. Additionally, concerns regarding repairability, recyclability, and end-of-life disposal require comprehensive solutions [1].

The complexity and cost of physical testing in the automotive sector has led to extensive reliance on numerical simulation tools for new developments. This trend is further amplified by emerging regulations that increasingly favour virtual homologation methodologies, where physical testing of evaluated load cases may not be required [2]. This transition is facilitated by advances in Human Body Model development, which replace traditional virtual dummies in simulations, providing more accurate assessments of potential injury mechanisms.

When considering new materials for automotive production, compatibility with existing -or readily implementable- manufacturing processes is essential [1]. Similarly, efficient and reliable simulation tools are required to maintain reasonable development costs while ensuring integration with established procedures. Engineering tools for developing components with novel materials must be sufficiently accurate to ensure predictability while remaining versatile enough for incorporation into conventional development workflows. When these criteria are satisfied, innovative features such as advanced materials can be successfully implemented.

Currently, automotive component development is predominantly conducted using Computer-Aided Engineering (CAE) tools, with the Finite Element (FE) method being one of the most widely adopted methodologies. This approach necessitates comprehensive material characterisation to ensure accurate prediction of material behaviour under diverse loading scenarios.

In this context, a Building Block Approach is conducted through parallel experimental testing and FE simulation campaigns, progressing from material coupons to full-vehicle crash conditions [2]. This methodology enables virtual testing of numerous configurations, thereby reducing the number of required physical tests while enhancing the efficiency of development and validation of numerical models used in virtual homologation methods. A schematic representation of this approach applied to automotive development is illustrated in Figure 1.

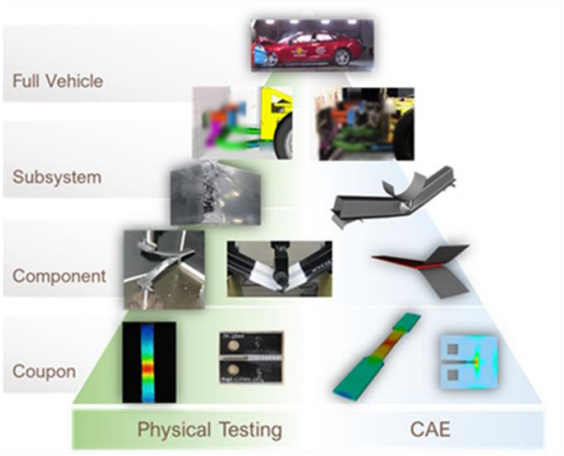

Fig.1: Diagram of Building Block Approach in automotive framework [3].

The commercially available software LS-DYNA is extensively utilised in the automotive industry and has proven to be a powerful tool for FE simulation of crash-related events, facilitating the development of new vehicles and components. LS-DYNA offers a comprehensive range of constitutive models for representing various materials that influence occupant safety. For certain material classes, it demonstrates advanced capabilities, such as the SAMP model for non-isochoric plasticity and the GISSMO damage model [4, 5].

For composite materials, LS-DYNA provides several material models suitable for crash simulations. Despite this, limitations persist for the simulation of fabric-reinforced composite materials, widely employed in the automotive sector due to their superior drapeability and impact energy absorption characteristics. Consequently, there remains a clear need for more efficient and predictive simulation methodologies.

This work presents a constitutive model specifically designed for the simulation of fabric-reinforced composite materials in LS-DYNA. The proposed model builds upon the framework presented in [7], which shares fundamental features with Material 262 (**`*MAT262`**) from the LS-DYNA libraries. It incorporates efficient failure envelopes and the enhancements presented in[3], while introducing additional features to address the specific requirements of fabric-reinforced composites under crushing events.

The proposed model is implemented as a User-Defined Material (UMAT) in LS-DYNA v15, enabling direct comparison with the enhanced (**`*MAT262`**) from the LS-DYNA libraries.

1.1 Fabric composite simulation in LS-Dyna

LS-DYNA offers several material models for simulating composite materials suitable for crash simulations.

Material 58 (***MAT58**) represents the most established option for fabric-reinforced composites. This model employs phenomenological laws that focus less on identifying specific damage mechanisms and more on capturing their combined effect on material response, employing damage initiation based on a maximum stress criterion [6]. Following initiation, residual stress and elimination strain parameters can be defined; however, this model lacks the capability to specify fracture toughness at the first peak or establish a controlled post-peak damage evolution. Furthermore, it does not implement Fracture Toughness regularisation with respect to element size, resulting in mesh-dependent structural responses. This limitation creates difficulties when modelling components experiencing extensive progressive damage, such as energy-absorbing crush tubes.

Materials 261 and 262 are defined for Unidirectional (UD) reinforced materials and are based on micromechanical approaches. Failure envelopes aim to predict the specific mechanisms causing material degradation. This approach results in sophisticated damage formulations that may be computationally intensive for large-scale models with refined meshes, leading to extended simulation times.

Material 262 addresses several limitations observed in Material 58. Based on the model published by Maimí et al. (2006) [6], it implements a bilinear damage law for fibre-related mechanisms. Each damage mechanism incorporates Bažant's Crack-Band model, thereby reducing mesh dependency during single crack propagation. However, the original version of Material 262 exhibits certain limitations, including linear plasticity for in-plane shear mechanisms and coupling effects in damage evolution that can lead to premature failure under complex loading conditions, particularly in the axial crushing of safety-critical components.

Beyond these specific characteristics, both material models demonstrate limited predictive capability when components are subjected to combined bending and crushing stresses. In [3], the authors proposed modifications to Material 262 to improve correlation under these conditions, which are representative of automotive crash scenarios. These enhancements included an advanced failure envelope, coupling of damage with out-of-plane mechanisms, and refinements to the softening behaviour. The proposed improvements significantly enhanced predictability for automotive crash simulations involving composite components and have been incorporated into Material 262 from the LS-DYNA r15 release onwards.

For the simulation of fabric-reinforced composites, available options include using Material 58 with its inherent limitations in damage definition. Other option is to use Material 262, but since this formulation is specific for UD-reinforced composites, each ply in the fabric material needs to be split into two equivalent [0º,90º] unidirectional plies. Figure 2 provides a schematic representation of this ply-splitting technique.

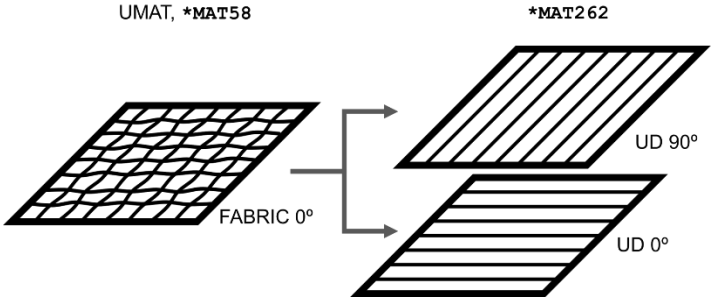

Fig.2: Schematic representation of laminate split.

While the latter approach leverages Material 262's damage prediction capabilities, it introduces several disadvantages:

- The laminate's bending response becomes dependent on material orientation.
- The number of integration points in the model effectively doubles.
- The material card creation process becomes significantly more complex and time-consuming.
- Fabric-specific failure mechanisms and damage propagation patterns cannot be directly represented.

These factors contribute to increased simulation duration and necessitate precise knowledge of principal loading directions for appropriate laminate orientation.

2 Model description

2.1 Proposed Material Model

To address the limitations previously discussed, a new material law is proposed for the simulation of fabric-reinforced composite materials. This constitutive model is based on the framework presented in [7], with significant enhancements specifically designed for application in the automotive industry.

Building upon the established knowledge from Materials 58 and 262, whilst avoiding their respective limitations, the proposed model incorporates the following key features:

- Phenomenological-based laws to ensure computational efficiency.
- Direct representation of fabric-specific behaviour using mainly Measurable Physical properties.
- Fracture toughness regularisation implemented across all damage mechanisms to mitigate mesh dependency.
- Controlled post-peak stress evolution for accurate representation of crushing forces and large deformations.
- Optional inelastic damage formulation to improve prediction of component final deformation and rebound forces after impact events.
- Optimised computational performance for large-scale automotive crash simulations.

This comprehensive approach enables more accurate prediction of fabric-reinforced composite behaviour under the complex loading conditions characteristic of automotive crash scenarios, whilst maintaining computational efficiency. The direct modelling of fabric materials eliminates the need for equivalent UD approximations, thereby streamlining the material characterisation process and reducing potential sources of error in damage evolution assessment.

2.2 Constitutive model

The constitutive behaviour of the material is defined by the scalar function of the complementary free energy density ($\mathcal{G}$). For the presented model, it is defined as:

$$\mathcal{G} = \frac{(\sigma_1)^2}{2(1-d_1)E_1} + \frac{(\sigma_2)^2}{2(1-d_2)E_2} + \frac{(\sigma_4)^2}{2(1-d_4)G_{12}} - \frac{(1-d_1)(1-d_2)\nu_{12}}{(1-d_1)E_1}\sigma_1\sigma_2 + \sigma_4\varepsilon_4^p \tag{1}$$

where $\sigma_1, \sigma_2, \sigma_4$ are the components of the stress tensor, E_1, E_2 are the elastic moduli, G_{12} is the in-plane shear modulus, ν_{12} is the in-plane Poisson's ratio, ε_4^p is the in-plane shear plastic strain, and d_1, d_2, d_4 are the components of the damage tensor.

The indexing convention used throughout this formulation follows standard practice for fabric reinforced composites, where:

- Index 1 defines the principal direction (corresponding to fibre warp direction)
- Index 2 defines the transverse direction (corresponding to fibre weft direction)
- Index 4 defines the in-plane shear component

This formulation explicitly accounts for both elastic degradation through the damage variables d_i and inelastic deformation through the plastic strain term ε_4^p. The latter is particularly important for accurately capturing the nonlinear shear response characteristic of fabric-reinforced composites.
The irreversibility of the damage process at each material point is ensured by a positive rate of evolution of the energy dissipated (Ξ):

$$\Xi = \dot{\mathcal{G}} - \dot{\sigma}:\varepsilon = \frac{\partial \mathcal{G}}{\partial \varepsilon^p}\dot{\varepsilon^p} + \frac{\partial \mathcal{G}}{\partial d_1}\dot{d_1} + \frac{\partial \mathcal{G}}{\partial d_2}\dot{d_2} + \frac{\partial \mathcal{G}}{\partial d_4}\dot{d_4} + \left(\frac{\partial \mathcal{G}}{\partial \sigma} - \varepsilon\right):\dot{\sigma} \geq 0 \tag{2}$$

For thermodynamic consistency, damage variables must increase monotonically, and the evolution of in-plane plasticity must be in concordance with its related stress (σ_4). This is ensured if:

$$\left(\frac{\partial \mathcal{G}}{\partial \sigma} - \varepsilon\right) : \dot{\sigma} = 0 \tag{3}$$

Then, the strain field becomes determined by:

$$\varepsilon = \frac{\partial \mathcal{G}}{\partial \sigma} = \mathbf{H} : \sigma + \varepsilon^p \tag{4}$$

where $\mathbf{H}$ is the compliance tensor. Since FE software works in small strain increments, inverting Eq. 4, the stresses can be computed:

$$\sigma = \mathbf{S}(\varepsilon - \varepsilon^p) \tag{5}$$

where $\mathbf{S}$ is the stiffness matrix. Using Voigt notation, it is defined as

$$\mathbf{S} = \begin{bmatrix} \Delta(1-d_1)E_{11} & \Delta(1-d_1)E_{11}(1-d_2)\nu_{21} & 0 & 0 & 0 & 0 \\ \Delta(1-d_2)E_{22}(1-d_1)\nu_{21} & \Delta(1-d_2)E_{22} & 0 & 0 & 0 & 0 \\ 0 & 0 & 0 & 0 & 0 & 0 \\ 0 & 0 & 0 & (1-d_4)G_{12} & 0 & 0 \\ 0 & 0 & 0 & 0 & G_{13} & 0 \\ 0 & 0 & 0 & 0 & 0 & G_{23} \end{bmatrix} \tag{6}$$

Where Δ is defined as:

$$\Delta = \frac{1}{1 - \left((1-d_1)\nu_{12}(1-d_2)\nu_{21}\right)} \tag{7}$$

The configuration of fabric-reinforced composites commonly results in different mechanical responses under tension and compression loading. This tension-compression asymmetry is particularly pronounced due to the specific architecture of woven reinforcements and their interaction with the matrix material. To account for this phenomenon, the constitutive model incorporates strain-dependent elastic moduli:

$$\begin{aligned} E_i &= E_{iT} \text{ when } \varepsilon_i > 0 \text{ and} \\ E_i &= E_{iC} \text{ when } \varepsilon_i < 0 \end{aligned} \tag{8}$$

where the subindexes T and C denote tension and compression, respectively, for $i = [1,2]$.

2.3 Inelasticity onset and evolution

2.3.1 Shear isotropic hardening

When loaded under in-plane shear stress, fabric-reinforced composites typically exhibit significant nonlinear behaviour, characterized by large strain development. This nonlinearity stems from a combination of mechanisms, including matrix plasticity, progressive fibre reorientation (scissoring effect), and void micro-cracking at the fibre-matrix interface. To capture these phenomena, an advanced isotropic plasticity formulation is implemented in the constitutive model:

$$F_{12} = \left|\tilde{\sigma}_{12}{}^T\right| - \left(S_L + \varsigma_e\left(1 - e^{-\left|\varsigma_{Te}\varepsilon_{12}^i\right|}\right) + \varsigma_l\varepsilon_{12}^i + \varsigma_c{\varepsilon_{12}^i}^2\right) \tag{9}$$

where ε_{12}^i is the isotropic hardening variable, that allows to compute the plastic strain evolution: $\dot{\varepsilon_{12}^p} = \dot{\varepsilon_{12}^i}\text{sign}(\varepsilon_{12}^e)$.

This quadratic exponential formulation provides significant flexibility in representing the complex shear response of fabric-reinforced composites, including the characteristic scissoring effect observed prior to

failure. The parameter S_L represents the initial yield stress, while ς_e ς_{Te}, ς_l and ς_c are material-specific fitting parameters that define the isotropic hardening law.

All parameters in this formulation can be systematically identified from standardised off-axis tests, particularly tensile tests on $[\pm 45^{\cdot}]_{ns}$ specimens in accordance with ASTM D3518. This approach ensures that the model accurately captures the distinctive nonlinear shear behaviour of fabric-reinforced composites, which significantly influences energy absorption during crash events. Figure 3 shows an example of the law that can be obtained.

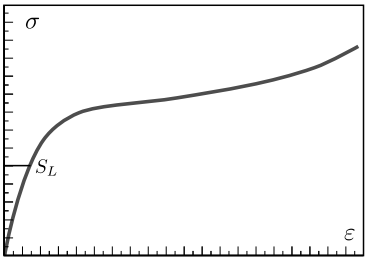

Fig.3: Representative shear stress-strain curve for a fabric-reinforced composite, showing the characteristic nonlinear response captured by the model.

2.3.2 Damage mechanisms

The proposed model utilizes a comprehensive damage characterization framework with five independent damage variables to accurately represent the various degradation mechanisms in fabric-reinforced composites. This approach allows for separate treatment of tension and compression damage in the principal material directions, recognizing the fundamentally different failure mechanisms that occur under these loading conditions.

Then,
- d_{1T} and d_{2T} are used for the tensile damage of the principal directions
- d_{1C} and $d_{2C}$are used for the compression damage of the principal directions

Finally,
- d_4 is used for the consideration of shear damage.

This formulation enables the model to capture the distinct effects of different damage mechanisms on the composite's mechanical response. For instance, tension damage in woven fabrics is primarily characterized by progressive fibre breakage and interfacial debonding, while compression damage typically involves fibre kinking, microbuckling, and matrix crushing.

A key advantage of this separate treatment of tension and compression damage is the ability to model crack closure mechanisms. When a previously tension-damaged region is subsequently subjected to compression, the physical closure of microcracks can restore the material's compressive load-bearing capacity.

2.3.3 Damage activation functions

The elastic domain in the proposed constitutive model is bounded by five distinct failure surfaces, each corresponding to a specific damage mechanism in the fabric-reinforced composite ($1T, 2T, 1C, 2C$ and 4).

Each failure surface is mathematically defined by a damage activation function F_M, which takes the general form:

$$F_M = \phi_M - r_M \leq 0 \quad M = 1T, 2T, 1C, 2C, 4 \tag{10}$$

where ϕ_M represents the loading function associated with mechanism M, and r_M is the corresponding internal variable that tracks the historical maximum value of ϕ_M. This formulation ensures that damage evolution satisfies the irreversibility condition required for thermodynamic consistency.

The material response at a given integration point follows these principles:

- While $F_M < 0$, the material exhibits pure elastic behaviour for mechanism M.
- When $F_M = 0$ and $\dot{F_M}\big|_{r_M=0} \leq 0$, the material undergoes elastic unloading or neutral loading.
- When $F_M = 0$ and $\dot{F_M}\big|_{r_{M=0}} > 0$, damage evolution occurs for mechanism M.

During damage evolution, the failure surface expands such that the current stress state remains on the evolving surface, following the consistency condition:

$$\dot{\phi_M} = \dot{r}_M \text{ when } F_M = 0 \text{ and } \dot{F_M}\big|_{r_{M=0}} > 0 \tag{11}$$

This rate-independent damage formulation ensures that the internal variables r_M are non-decreasing functions of time, preserving the thermodynamic consistency of the model. The evolution of each damage variable d_M is then determined based on the corresponding internal variable r_M through specific damage evolution laws, which will be detailed in next sections.

2.3.4 Loading functions

The loading functions define the elastic domain of the material in the effective stress space $\tilde{\sigma}_i$, and thus depend on both the strain tensor and material properties. For the proposed constitutive model, a maximum stress criterion with stress interaction terms has been adopted to account for damage onset and propagation in fabric-reinforced composites.

The loading functions are defined as:

$$\begin{aligned} \phi_{1T} &= \frac{\langle \tilde{\sigma}_{11} \rangle}{X_{1T}} \quad ; \quad \phi_{1C} = \frac{\langle -\tilde{\sigma}_{11} \rangle + \eta_{1T}\tilde{\sigma}_{22} + \eta_{1S}\tilde{\sigma}_{12}}{X_{1C}} \\ \phi_{2T} &= \frac{\langle \tilde{\sigma}_{22} \rangle}{X_{2T}} \quad ; \quad \phi_{2C} = \frac{\langle -\tilde{\sigma}_{22} \rangle + \eta_{2T}\tilde{\sigma}_{11} + \eta_{2S}\tilde{\sigma}_{12}}{X_{2C}} \\ \phi_4 &= \frac{|\tilde{\sigma}_{12}|}{X_4} \end{aligned} \tag{12}$$

where $\tilde{\sigma}$ is the effective stress tensor, defined as $\tilde{\sigma} = \mathbf{S}_0 : \varepsilon^e$. Here, ε^e is the elastic strain tensor and $\mathbf{S}_0$ corresponds to the undamaged stiffness tensor, obtained from Equation (6) with all damage variables $d_M = 0$. The Macaulay brackets $\langle \cdot \rangle$ return the positive part of their argument, ensuring that criteria are only activated under its correspondent T or C stress states.

The parameters $X_{1T}, X_{1C}, X_{2T}, X_{2C}$ and X_4 represent the ultimate strengths for each damage mechanism, while $\eta_{1T}, \eta_{1S}, \eta_{2T}$ and η_{2S} are non-dimensional coupling factors that define the biaxial interaction behaviour [8,9]. These parameters can be systematically identified from the failure envelope, which is typically determined experimentally through biaxial tests on thickness-tapered cruciform specimens [8].

A distinctive feature of this formulation is the incorporation of stress interaction terms in the compressive damage mechanisms. These terms account for the physical phenomenon where the presence of transverse or shear stresses can significantly alter the compressive strength of the material. Specifically:

- Transverse compressive stress can constrain fibre microbuckling, thereby increasing the effective compressive strength along the principal direction.
- In-plane shear stress promotes fibre misalignment, facilitating the formation of kink bands and thus reducing the compressive strength.

These micromechanical interactions are particularly important for accurately predicting the complex failure modes observed in fabric-reinforced composites during automotive crash events, where

multiaxial stress states are common. In contrast, the tensile failure mechanisms are primarily controlled by the effective stress in the corresponding direction, with minimal influence from other stress components.

Figure 4 provides a graphical representation of the loading functions implemented in the proposed constitutive model. The left figure illustrates the failure envelope in the principal stress space ($\sigma_1 - \sigma_2$), while the right figure shows the interaction between principal stresses and shear stress.

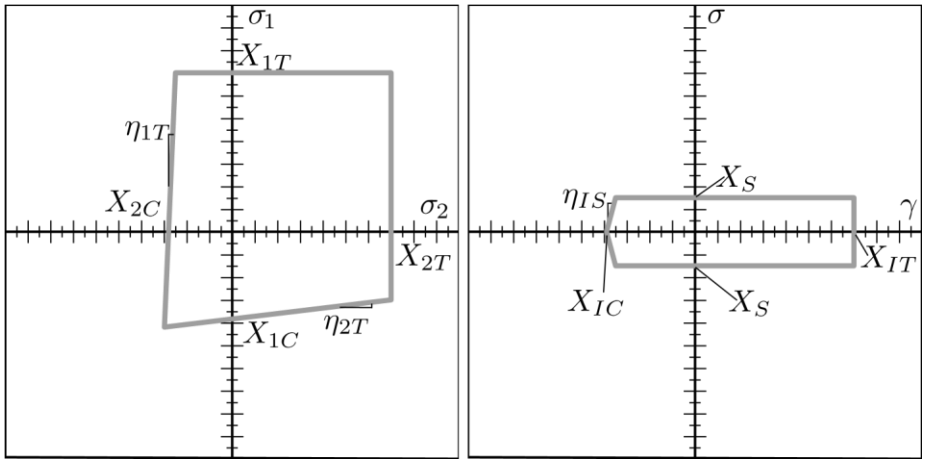

Fig.4: Failure criteria for the principal directions(left) and for the principal direction with the shear plane (right).

2.3.5 Damage thresholds

The internal variables r_M serve as damage propagation thresholds, establishing the maximum value that loading functions can reach before additional damage occurs. When a loading function exceeds its corresponding threshold, damage evolution is triggered, and the threshold value is updated accordingly.

A key aspect of the proposed model is its treatment of the interaction between tensile and compressive damage mechanisms. The internal variables associated with tensile mechanisms (r_{1T} and r_{2T}) are defined by the historical maximum of both tensile and compressive loading functions in the corresponding direction. This approach captures the physical reality that compressive failure mechanisms (such as kink band formation) can significantly degrade the material's subsequent tensile performance.

In contrast, the internal variables for compressive mechanisms (r_{1C} and r_{2C}) are influenced solely by their corresponding compressive loading functions. This formulation implements the crack closure mechanism discussed previously, where prior tensile damage has a limited effect on subsequent compressive performance due to the physical closure of microcracks under compression.

The evolution of internal variables r_M is computed under an explicit integration scheme as follows:

$$\begin{aligned} r_{1T} &= \max_{s=0,t}\{1, \phi_{1T}^s, \phi_{1C}^s\} \quad ; \quad r_{1C} = \max_{s=0,t}\{1, \phi_{1C}^s\} \\ r_{2T} &= \max_{s=0,t}\{1, \phi_{2T}^s, \phi_{2C}^s\} \quad ; \quad r_{2C} = \max_{s=0,t}\{1, \phi_{2C}^s\} \\ r_4 &= \max_{s=0,t}\{1, \phi_4^s\} \end{aligned} \tag{13}$$

As can be observed, the internal variables take an initial value of 1 when the material is undamaged (i.e. $d_M = 0$). When the loading functions increase beyond that value damage begins, and the internal variables are increased to define the new threshold for damage evolution. With the new value for r_M, the corresponding damage variables are updated, reflecting the loss of stiffness caused by the new degradation state in the material.

2.3.6 Damage variables

The constitutive model employs a set of five damage variables to quantify the progressive stiffness degradation in the material. These damage variables are derived from the internal variables r_M through carefully formulated damage evolution laws that capture the complex failure behavior of fabric-reinforced composites.

A key innovation in the proposed model is the multi-stage damage evolution approach, illustrated in Figure 5. This approach enables accurate representation of the distinct phases of damage progression observed in experimental testing of fabric composites, from initial failure through progressive degradation to residual strength.

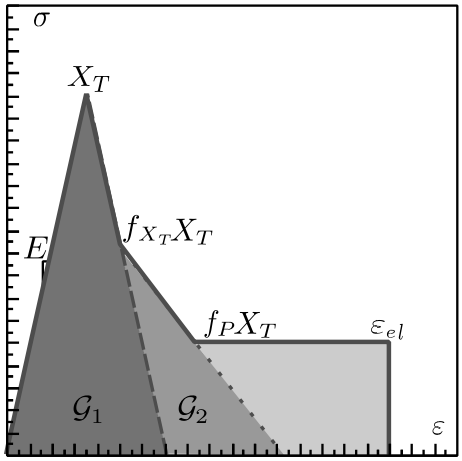

Fig.5: Schema of Representative Constitutive law and the parameters that define it.

For a piecewise linear evolution of stress with strain, the damage variables are defined by the general formulation:

$$d_M = \frac{1 - \left(\frac{A_M^V}{E_M}\right) r_M X_M - B_M^V}{r_M X_M} \tag{14}$$

where A_M^V and B_M^V represent the slope and the vertical intercept of the stress-strain response in the active damage stage. The index V defines the stage of degradation, being 1 for peak damage, 2 for post-peak damage and 3 for residual stress. These parameters vary according to three distinct stages of degradation, each corresponding to specific physical mechanisms in fabric-reinforced composites:

Peak stage
This stage initiates at the ultimate strength of the material (X_M) and represents the primary failure of load-bearing fibres. It is characterized by a high ultimate strength and a relatively steep negative slope in the stress-strain response. The rapid decrease in load-carrying capacity corresponds to the progressive breakage of primary fibres in tension, or the formation of initial kink bands in compression. The energy dissipated during this stage is primarily associated with the creation of new fracture surfaces.

Post-peak stage
This intermediate stage represents secondary degradation mechanisms with a less severe slope than the initial failure. In tensile loading, it corresponds to the breakage of remaining fibres and the initiation of fibre pull-out processes. In compression, it represents the failure of secondary fibres after initial kink band formation and the broadening of existing kink bands. This stage is crucial for accurately modelling the progressive collapse of composite structures in crash simulations, as it governs the transition from initial failure to residual load-carrying capacity.

Residual stress stage
The final phase of material degradation maintains an optional non-zero stress level despite significant deformation. For tensile mechanisms, this stage primarily captures the pull-out resistance of broken

fibres embedded in the matrix. For compressive mechanisms, it represents the frictional resistance and debris compaction within fully developed kink bands. The accurate modelling of residual stress is particularly important for crash simulations, as it significantly influences force transmission during component crushing and prevents premature element deletion.

The parameters A_M^V and B_M^V in each stage are calculated parameters are computed from the material properties, to satisfy two essential requirements:

- Ensure stress continuity at the transition between damage stages
- Preserve the fracture energy dissipation regardless of mesh refinement

This multi-stage approach provides independent control of the damage evolution trajectory for each mechanism, enabling accurate representation of the distinct failure behaviours observed in warp, weft, and shear directions while ensuring mesh-objective results through proper scaling of energy dissipation with element characteristic length.

A distinctive feature of the model is the ability to define customized inelastic damage in the post-peak and residual stress stages. This flexibility allows for various material responses, including full damage (stiffness decays to zero), fully plastic-like behaviour (constant residual stiffness), or intermediate behaviours. This capability is especially valuable for representing the diverse failure characteristics of different polymer matrix systems used in automotive composites, enhancing the model's applicability across a wide range of fabric-reinforced materials. This algorithm will be detailed in next section.

2.3.7 Inelastic Damage

A critical limitation of conventional damage mechanics approaches for composite materials is their inability to accurately represent permanent deformation following load removal. While composite materials typically exhibit significant residual deformation after loading beyond the damage threshold, standard constitutive models implement damage solely as a stiffness reduction. This formulation causes finite elements to unrealistically recover their original geometry upon unloading, resulting in artificial energy storage and excessive rebound forces.

This phenomenon is particularly problematic in automotive crash simulations, especially for scenarios involving pedestrian impact, where precise representation of impact and rebound mechanics is essential for regulatory compliance assessment. The artificially elevated rebound forces can lead to significant overestimation of secondary impact accelerations and unrealistic component deformation recovery.

To address this limitation, the proposed constitutive model incorporates an innovative inelastic damage formulation. This algorithm application starts at post-peak stage and introduces a permanent strain component that remains after stress release. The user can specify a recovery factor that defines the ratio between elastic (recoverable) and inelastic (permanent) strain, allowing for precise calibration of the material's unloading behaviour.

Figure 6 illustrates the effect of the inelastic damage formulation on the load-unload response of a composite element. The conventional elastic damage approach (dashed line) shows complete strain recovery upon unloading, while the inelastic damage approach (solid line) maintains a permanent deformation, more accurately representing the actual behaviour of fabric-reinforced composites.

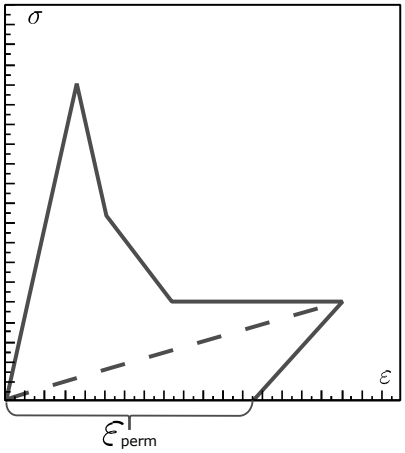

Fig.6: Comparison of conventional elastic damage and inelastic damage approaches for single element

This formulation offers several advantages for automotive crash simulation:

- Improved prediction of component final shape after impact
- More realistic energy dissipation during unloading phases
- Reduced artificial rebound forces and secondary accelerations
- Enhanced correlation with physical test results for multi-impact scenarios

2.3.8 Effective Poisson

A significant limitation in conventional constitutive models for composites is their treatment of Poisson effects during damage evolution. Standard approaches calculate damage activation based on effective (undamaged) stress tensors, using the undamaged stiffness matrix. This methodology can lead to substantial overestimation of material resistance in certain loading scenarios due to unrealistic Poisson-induced strains in the damaged material.

This phenomenon is particularly evident in biaxial tension-compression loading cases, as illustrated in Figure 7. It becomes maximized where the tension strain in direction 1 is applied at the same time than a compression strain in direction 2 with modulus equal to the Poisson ratio.

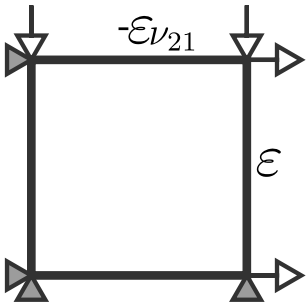

Fig.7: Single element loaded in biaxial tension-compression conditions.

In conventional models such as ***MAT262**, the presented load case into leads to $\tilde{\sigma}_2 = 0$ as shown in Eq. 15.

$$\tilde{\sigma}_2 = E_{22}\nu_{12}\varepsilon_1 + E_{22}\varepsilon_2 = 0 \quad \text{if} \quad \varepsilon_2 = -\nu_{12}\varepsilon_1 \tag{15}$$

This mathematically convenient cancellation creates a physically unrealistic situation where damage is not detected in direction 2, despite potentially significant compressive strains that may exceed the material's compressive strength. This limitation can lead to severe overestimation of structural integrity in complex loading scenarios typical of automotive crash events.

The proposed constitutive model addresses this limitation by implementing damage effects directly on the Poisson ratio when calculating the effective stress tensor. This approach ensures that Poisson-induced strains properly contribute to damage detection and evolution. The modified effective stress calculation becomes:

$$\tilde{\sigma}_2 = E_{22}(1 - d_1)\nu_{12}\varepsilon_1 + E_{22}\varepsilon_2 \neq 0 \tag{16}$$

where d_1 is the damage variable in direction 1. As damage develops in direction 1, the effective Poisson contribution diminishes, preventing the artificial cancellation of stresses in direction 2.

In Figure 8, a numerical example demonstrating the significant impact of this formulation is shown, by comparing the proposed model with the conventional ***MAT262** approach. Both materials have identical compressive strength parameters ($X_{2C} = 600$ MPa), yet ***MAT262** (grey line) allows stress to reach nearly triple this value before detecting damage. In contrast, the proposed model correctly identifies damage onset at the specified strength threshold (black line).

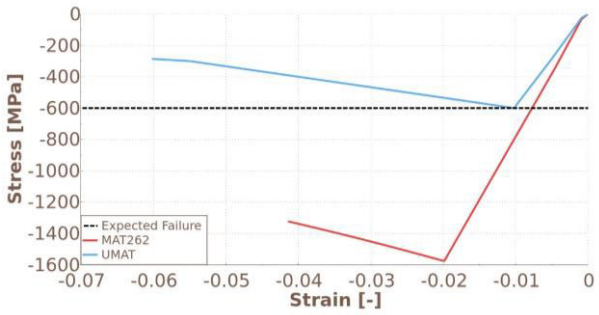

Fig.8: Stress in compression (direction 2) for the biaxial case depicted in Figure 7.

3 Numerical Models

The numerical simulations in this work were performed using LS-DYNA r15.02 to leverage the latest updates in the implementation of ***MAT262**, which represents the current methodology adopted at IDIADA for the development of composite structures.

Three distinct material modelling approaches were evaluated for the composite material definition:

- Proposed constitutive model (implemented via UMAT)
- UD-equivalent ***MAT262** implementation
- ***MAT58** implementation

The proposed constitutive model was implemented through a UMAT routine written in FORTRAN, which allows for direct representation of fabric-reinforced composites. For the standard ***MAT262** simulations, each fabric ply was represented as two unidirectional plies in a $[0º, 90º]$ configuration, following the conventional approach described in Section 1.1.

3.1 Simulation methodology

The explicit solver was selected for all simulations to accommodate the significant non-linearities in both geometry and material response that characterise crushing events. This approach is particularly appropriate for automotive crash simulations, where high deformation rates and complex contact conditions are prevalent.

Composite materials were modelled using shell elements with fully integrated formulation (ELFORM 16) to avoid the introduction of artificial energies caused by hourglass modes or element warping. This

formulation, though more computationally intensive than reduced integration alternatives, provides superior accuracy for the complex damage mechanisms being investigated.

The modelling approach was adapted according to simulation scale:

- **Coupon-level tests**: Composites were simulated using a single-shell definition with the complete laminate stacking sequence defined within the shell section properties.
- **Component-level tests**: The laminate was divided into multiple shell elements through the thickness, with inter-ply behaviour represented by cohesive elements to capture delamination effects.

Auxiliary equipment such as impactors, loading devices, and clamping fixtures were modelled using rigid body definitions (`*MAT20`) where required in the simulation setup.

3.2 Mesh considerations

To maintain consistency with standard automotive industry practices, a characteristic element length of 4 mm was employed for most simulations. This element size represents a balance between computational efficiency and sufficient resolution to capture the key deformation and failure mechanisms.

Exceptions to this mesh size were implemented only where geometrical constraints necessitated refinement:

- Compact Compression test: $l_e = 1.4$ mm
- Holed specimens: $l_e = 1.0$ mm

Importantly, identical material parameter definitions were maintained across all mesh densities. This approach ensured that the constitutive model's mesh objectivity features were properly evaluated, confirming its capability to accurately predict material behaviour despite variations in discretisation refinement, a critical requirement for practical automotive applications where mesh density often varies across a single component.

4 Results

In this section, the correlation results for coupon and component simulation with the different approaches are shown.

4.1 Coupon tests

The composite materials evaluated in this work comprise carbon fibres in a twill woven configuration embedded in an epoxy matrix. A comprehensive experimental coupon testing campaign was conducted and subsequently simulated to determine material properties and calibrate virtual performance. From this dataset, the most relevant tests for predicting crushing behaviour in tubular structures have been selected for presentation.

This section presents simulation results for the following coupon tests:

- In-plane shear response (ASTM D3518)
- Flexural properties (ASTM D790)
- Open-hole tension and compression response
- Compact compression behaviour

These tests were selected to systematically evaluate the constitutive model's ability to predict key deformation and failure mechanisms relevant to crash energy absorption, including:

- Non-linear shear behaviour
- Bending response with mixed tensile-compressive loading

- Stress concentration effects and damage propagation
- Stable crack growth under compressive loading

For each test configuration, results from the three modelling approaches (proposed UMAT, standard ***MAT262**, and ***MAT58**) are compared against experimental data to assess predictive capability.

4.1.1 In-plane shear test

The in-plane shear behaviour was evaluated using the standard ASTM D3518 test configuration, wherein woven fabric plies are aligned at $[\pm 45º]$ to the tensile loading direction. This orientation transforms the applied tensile load into an effective in-plane shear stress state within the material coordinate system, providing direct characterisation of the shear response.

Figure 9 presents the correlation between experimental data and the three numerical approaches.

Fig.9: Correlation In-plane shear D3518 test

Both the proposed UMAT implementation and ***MAT262** demonstrate accurate correlation of the in-plane shear plasticity and failure point detection. In the ***MAT262** results, a slight stiffening is observed near the end of the test, which advances the predicted failure strain, though this remains within the bounds of experimental variability.

The accurate prediction achieved with ***MAT262** leverages the enhanced capabilities introduced in recent versions, which allow for tabulated definition of shear stress-plastic strain relationships [3].

***MAT58** exhibits a fundamental limitation in this test, as it lacks a dedicated plastic strain mechanism for in-plane shear. Consequently, the entire non-linear response must be managed through damage evolution. This approach causes reduced correlation accuracy during the progressive development of non-linear deformation. Although the experimental damage initiation point is reasonably well predicted, the material model fails to capture the brittle failure observed in the physical specimens.

4.1.2 Bending test

The flexural behaviour was evaluated using the standard three-point bending configuration, with warp fibres aligned at $[0º]$ to the loading direction.

Figure 10 shows the correlation between experimental data and the three numerical approaches.

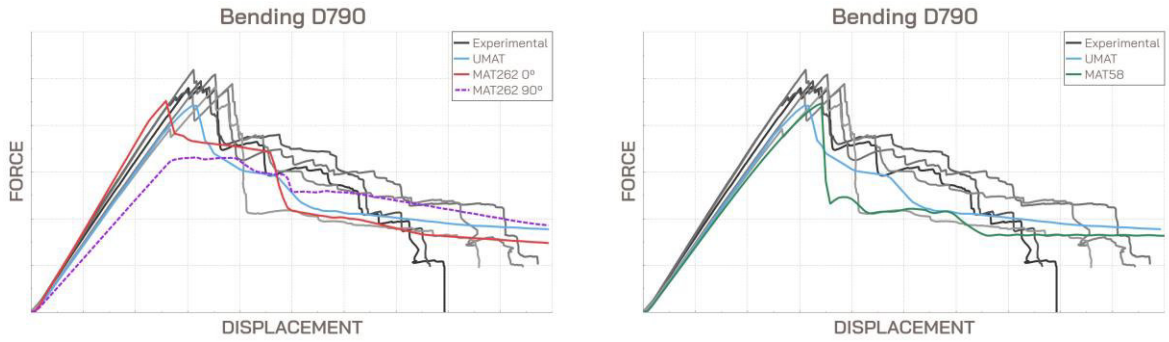

Fig.10: Correlation Bending D790. UMAT and experimental are compared with MAT262(left) and MAT58 (right)

The proposed UMAT demonstrates good correlation with experimental bending test results across the entire loading range.

The splitting of the fabric ply into unidirectional plies in ***MAT262** causes dependency on the laminate orientation. When simulated with the outer UD plies aligned at $[0º]$ to the loading direction, the model shows reasonable correlation, albeit with higher stiffness than experimentally observed. However, when the outer layers are oriented at $[90º]$ to the loading direction, the model significantly underestimates both stiffness and failure strength. This orientation-dependent behaviour represents a fundamental limitation of the equivalent UD approach discussed in Section 1.

***MAT58** shows proper correlation until the peak load, after which it exhibits an overly brittle failure response, underestimating the progressive damage observed in experimental results. The model does, however, accurately capture the residual force level after significant deformation.

4.1.3 Open Hole tests

These tests evaluate material performance with warp fibres aligned at $[0º]$ to the loading direction in both tension and compression modes. The central hole induces complex stress states around the discontinuity, providing insight into damage initiation and propagation under stress concentrations.

Figure 11 presents the correlation between experimental data and numerical predictions.

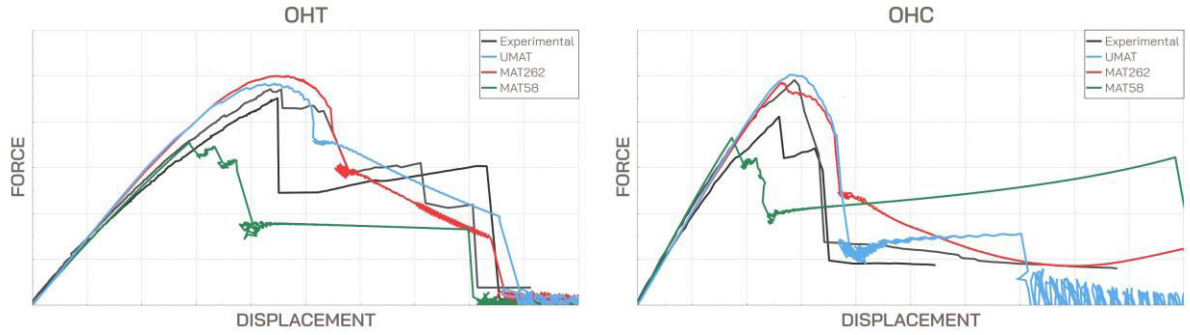

Fig.11: Results for Open hole tests under tension (Left) and compression (Right) loads.

In the open hole tests, significant delamination was observed experimentally prior to ultimate failure. The single-shell modelling approach employed in all three material models cannot explicitly capture this through-thickness failure mechanism, thus the loss of strain prior peak failure is not reproduced. Nevertheless, both UMAT and ***MAT262** accurately predict the maximum strength, whilst ***MAT58** underestimates the failure force in both tension and compression cases. The fracture energy regularisation algorithms implemented in both UMAT and ***MAT262** enable consistent predictions despite the refined mesh required around the hole, a capability not available in ***MAT58**.

In tensile tests, the single-shell modelling approach results in a smoother damage evolution in UMAT and ***MAT262** models compared to the more abrupt transitions observed experimentally under tensile loading. Despite the limitations observed, the ultimate failure strain is accurately captured by all three material models.

Under compressive loading, the peak damage is well reproduced by both UMAT and ***MAT262**, with only a slight overestimation of the strain at peak failure. In addition of the underestimation of peak force, ***MAT58** exhibits a non-physical increase in force near the end of the test, almost reaching the experimental maximum stress level. In this case, only UMAT shows final failure in the range of the experimental tests.

4.1.4 Compact Compression Test

The compact compression test evaluates stable crack growth in a pre-cracked thick specimen with warp fibres aligned at $[0º]$ to the loading direction. This test is particularly relevant for assessing the model's ability to predict progressive damage propagation under compressive loading.

Figure 12 presents the correlation between experimental and numerical results.

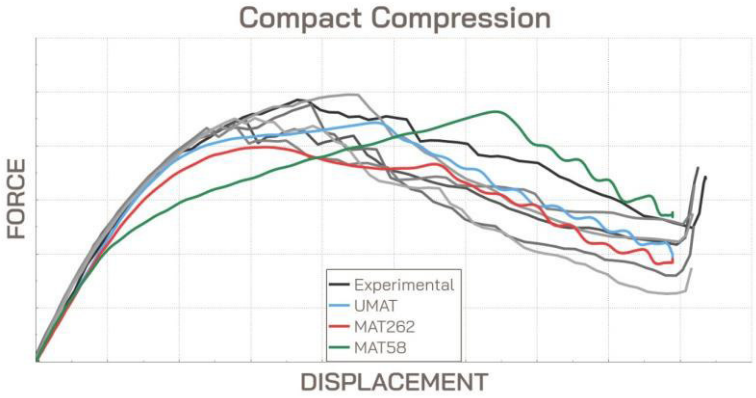

Fig.12: Results for Compact Compression test.

The proposed UMAT model demonstrates excellent correlation with experimental results, accurately capturing both the initial stiffness, maximum force, and subsequent progressive damage propagation. ***MAT262** shows good correlation of the crack propagation behaviour in the latter stages of the test, although it underestimates the maximum force.

***MAT58** exhibits delayed damage evolution, resulting in a later achievement of peak load compared to experimental observations. However, once damage initiates, the crack propagation pattern shows in reasonable agreement with experimental behaviour.

4.2 Component tests

To evaluate performance at the component level, square-section tubular structures were subjected to axial crushing using a flat impactor with a mass of 1300 kg. Impact speed was 22km/h for all cases except second repetition of tube 1A, where impact speed was increased to 32km/h. These tests represent realistic automotive crash energy absorption scenarios.

Two laminate configurations were evaluated:

- Tube 1A: All layers oriented at $[\pm 45º]$ relative to the tube's longitudinal axis
- Tube 1B: Mixed configuration with both $[\pm 45º]$ and $[0º]$ layers relative to the longitudinal axis

4.2.1 Tube 1A

Figure 13 presents the force-displacement response for the Tube 1A configuration.

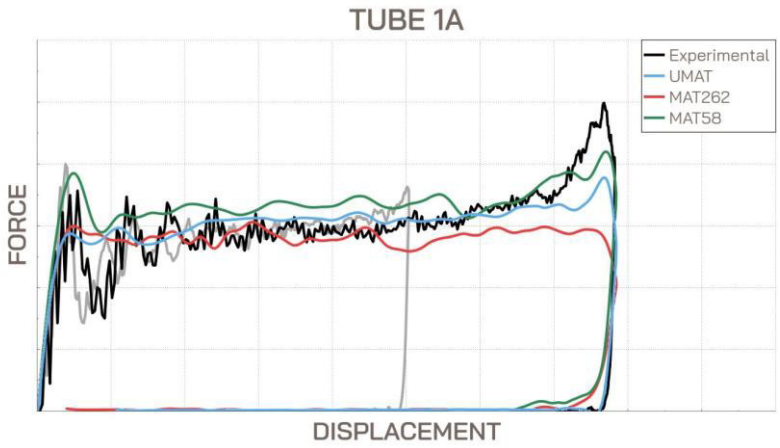

Fig.13: Force-Displacement results for tube 1A.

The proposed UMAT implementation demonstrates excellent correlation with the experimental crushing force, with only a slight underestimation of the final peak load. **`*MAT262`** shows good correlation up to the point where the experimental force begins to increase, beyond which the simulation fails to capture this trend. This discrepancy appears related to excessive element erosion in the **`*MAT262`** model.

`*MAT58` slightly overestimates the crushing force, consistent with the delayed damage progression observed in the coupon-level tests described in Section 4.1.1.

A particularly noteworthy finding emerges during the rebound phase, when the impactor begins to retract. Both **`*MAT58`** and **`*MAT262`** exhibit significantly higher rebound forces than experimentally observed, with greater displacement required to reach zero force due to their purely elastic damage formulation. In contrast, the inelastic damage mechanism implemented in the UMAT model enables accurate matching of the experimental rebound force profile.

4.2.2 Tube 1B

Figure 14 presents the force-displacement response for the Tube 1B mixed-orientation configuration.

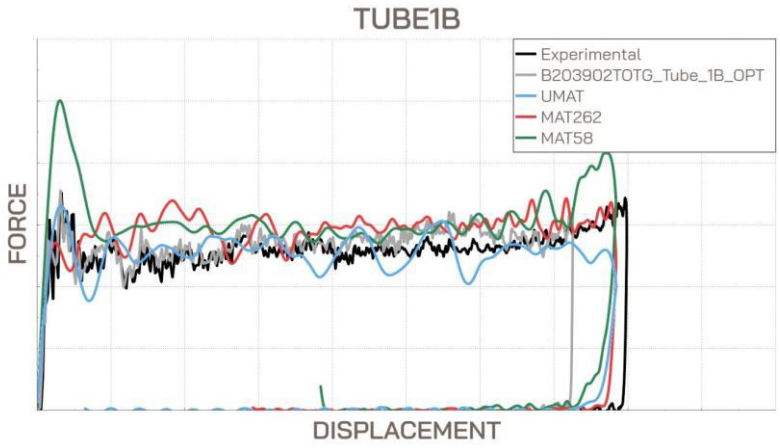

Fig.14: Force-Displacement results for tube 1B.

In this configuration, ***MAT58** overestimates the initial peak force, while all three models subsequently achieve satisfactory correlation levels suitable for automotive development. The UMAT model exhibits some oscillatory behaviour in the latter half of the test, attributed to the current absence of a SOFT parameter algorithm, which is implemented in both ***MAT58** and ***MAT262** to reduce the force sustained by elements once crushing has initiated. This feature will be implemented in future versions of the UMAT.

The element erosion observed in the ***MAT262** model results in better correlation of rebound forces for this configuration, though this apparent improvement stems from artificial elimination of material that would be problematic in full-vehicle simulations.

4.2.3 Deformation recovery comparison

Figure 15 illustrates the deformation patterns of Tube 1A at maximum displacement and after a prolonged relaxation period.

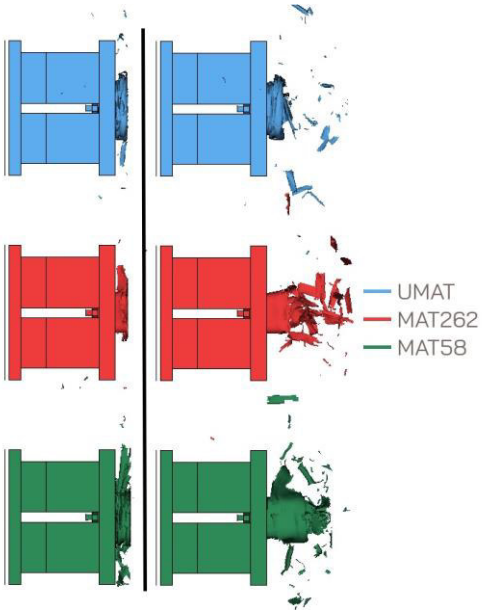

Fig.15: Deformation of Tube 1A at maximum displacement (left) and after prolonged relaxation (right).

After significant relaxation time, both ***MAT262** and ***MAT58** demonstrate substantial recovery towards the original tube geometry. ***MAT262** exhibits extensive element erosion and ejection of material fragments (Figure 17), resulting in unrealistic final geometry and excessive material loss. ***MAT58** (Figure 18) shows considerable elastic recovery, restoring approximately half of the original tube length.

In contrast, the inelastic damage algorithm implemented in the UMAT model produces a realistic final deformation pattern (Figure 16) that closely resembles the permanent deformation observed in physical testing.

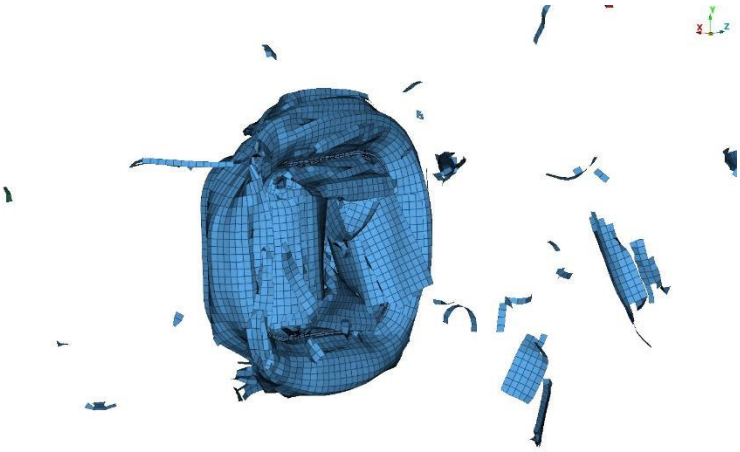

Fig.16: Final deformed shape of Tube 1A using the proposed UMAT model.

*Fig.17: Final deformed shape of Tube 1A using ***MAT262**, showing large element elimination.*

*Fig.18: Final deformed shape of Tube 1A using ***MAT58**, showing significant elastic recovery.*

5 Conclusions

This paper presents a novel constitutive model specifically designed for the simulation of fabric-reinforced composite materials in automotive crash applications. The model addresses several critical limitations in existing approaches while maintaining computational efficiency for full-vehicle simulations.

The proposed formulation builds upon previously published work by the authors, strategically incorporating the most advantageous features from established material models in LS-DYNA whilst introducing innovative capabilities. From ***MAT58**, the model adopts the direct representation of fabric-reinforced materials and an effective failure envelope formulation. From ***MAT262**, it incorporates advanced damage process management with proper fracture energy regularisation. Additionally, the model introduces several key innovations:

- A multi-stage damage evolution approach with controlled post-peak residual stress
- Integration of damage effects in the Poisson ratio calculation for effective stress determination
- An inelastic damage mechanism that accurately represents permanent deformation
- Direct fabric modelling capabilities without requiring equivalent unidirectional transformation

The comprehensive validation campaign, encompassing both coupon-level and component-level tests, demonstrates that the proposed constitutive model successfully overcomes significant limitations observed in currently available material models. The results show excellent correlation across diverse loading conditions, from in-plane shear and flexural response to complex crash behaviour in tubular structures Additionally, the material card creation process for the proposed law is significantly streamlined compared to *MAT262 equivalent UD modelling or *MAT58, as material properties are implemented more directly.

Whilst certain supplementary features, such as the softening of forces when neighbouring elements are damaged (**SOFT** parameter), are planned for future implementation in the user routine, the current formulation already demonstrates superior performance in predicting:

- Accurate force-displacement response during progressive crushing
- Realistic final deformed shapes after impact events
- Proper rebound force characteristics critical for secondary impact assessment

The inelastic damage mechanism shows marked improvements in both the representation of permanent deformation and the physical rebound behaviour of crashed components. This capability is especially valuable for multi-impact scenarios and pedestrian protection simulations, where realistic post-impact structural behaviour is essential for regulatory compliance assessment.

Future work will focus on implementing the SOFT parameter algorithm and further validating the model across a wider range of composite material systems and structural configurations.

6 Literature

[1] Liqin Yan and Hongtong Xu. Lightweight composite materials in automotive engineering:State-of-the-art and future trends. Alexandria Engineering Journal, 118:1–10, 2025.

[2] carhs.training. Safety Companion 2025. carhs, 2025.

[3] Alfredo Alameda, Alejandro Dominguez, Eduardo Martin-Santos, and Tomohiko Max Miura. Enhanced material model for composite crash performance at ply level. mat262 evolution. In Proceedings of the 2024 JSAE Annual Congress (Spring). JSAE, May 2024.

[4] Eduardo Martin-Santos, Lluis Martorell, Pablo Cruz, Megan Lobdell, and Hubert Lobo. Non-isochoric plasticity assessment for accurate crashworthiness CAE analysis. application to samp-1 and samp-light. Conference: 13th European LS-DYNA Conference, 2021

[5] Alejandro Dominguez, Pablo Cruz, Lluis Martorell, Adrián Ros, Eduardo Martin-Santos, Andrew Hall, Patrick Kelly, and Ilyasuddin Syed. Advanced plasticity & fracture for structural car body metals in crashworthiness CAE analysis: Samp-1 plus GISSMO. LS-DYNA Conference 2023.

[6] LS-DYNA R©KEYWORD USER'S MANUAL. VOLUME II: Material Models. Ansys, master@51f35439b edition, 10 2024.

[7] E. Martin-Santos, P. Maimí, E.V. González, and P. Cruz. A continuum constitutive model for the simulation of fabric-reinforced composites. Composite Structures, 111:122–129, 2014.

[8] C. G. Dávila, P. P. Camanho, and C. A. Rose. Failure criteria for FRP laminates. Journal of Composite Materials, 39:323–345, 2005.